Published in final edited form as:
J Am Chem Soc. 2013 November 6; 135(44): 16517–16525. doi:10.1021/ja407451c.

Translocation of cationic amphipathic peptides across the membranes of pure phospholipid giant vesicles

Sterling A. Wheaten, **Francis D.O. Ablan**, **B. Logan Spaller**, **Julie M. Trieu**, and **Paulo F. Almeida***
Department of Chemistry and Biochemistry University of North Carolina Wilmington, Wilmington, NC

Abstract

The ability of amphipathic polypeptides with substantial net positive charges to translocate across lipid membranes is a fundamental problem in physical biochemistry. These peptides should not passively cross the bilayer nonpolar region, but they do. Here we present a method to measure peptide translocation, and test it on three representative membrane-active peptides. In samples of giant unilamellar vesicles (GUVs) prepared by electroformation, some GUVs enclose inner vesicles. When these GUVs are added to a peptide solution containing a membrane-impermeant fluorescent dye (carboxyfluorescein), the peptide permeabilizes the outer membrane, and dye enters the outer GUV, which then exhibits green fluorescence. The inner vesicles remain dark if the peptide does not cross the outer membrane. But if the peptide translocates, it permeabilizes the inner vesicles as well, which then show fluorescence. We also measure translocation, simultaneously on the same GUV, by the appearance of fluorescently-labeled peptides on the inner vesicle membranes. All three peptides examined are able to translocate, but to different extents. Peptides with smaller Gibbs energy of insertion into the membrane translocate more easily. Further, translocation and influx occur broadly over the same period but with very different kinetics. Translocation across the outer membrane follows approximately an exponential rise, with a characteristic time of 10 minutes. Influx occurs more abruptly. In the outer vesicle, influx happens before most of the translocation. But some peptides cross the membrane before any influx is observed. In the inner vesicles, influx occurs abruptly sometime during peptide translocation across the membrane of the outer vesicle.

Keywords

Antimicrobial peptides; Cell-penetrating peptides; Dye release; Dye influx; Pore kinetics; GUVs

INTRODUCTION

The ability of cationic peptides to translocate across lipid membranes is a fundamental problem in physical biochemistry. Highly charged peptides should not be able to passively cross the nonpolar region of a lipid bilayer. And yet, they appear to do so. The discovery of cell-penetrating peptides (CPPs), which are able to enter live cells and even transport cargo with them, made it evident that these peptides have a vast potential in health applications (1). Some CPPs, such as penetratin (2) and TAT (3, 4), are derived from larger proteins; others, such as transportan 10 (TP10) (5–7), are chimeras based on amphipathic

*Corresponding author. Address: Department of Chemistry and Biochemistry, University of North Carolina Wilmington, Wilmington, NC 28403, USA, Tel: (910) 962-7300, Fax: (910) 962-3013. almei-dap@uncw.edu.

Notes
The authors declare no competing financial interests.

antimicrobial peptides; but others are oligomers (6-12 residues) of lysine or arginine. That oligoarginine is able to cross nonpolar phases in the presence of a counterion is well established (8–10). However, the question remains whether these peptides really cross the cell membrane through the lipid bilayer itself. Part of the uncertainty arises from the difficulty in measuring peptide translocation across a pure lipid membrane. Here we present a general method to measure peptide translocation and use it to examine three test cases.

In the course of preparation of giant unilamellar vesicles (GUVs) by electroformation, we observed that a small number of GUVs contained inner vesicles, of smaller but comparable diameters. The number of such giant vesicles containing inner ones is very small in each preparation, but their occurrence suggested a method to measure peptide translocation. The concept of the experiment is depicted in Figure 1. GUVs, with diameter $d \approx 100\ \mu$m, are prepared containing smaller GUVs, with $d \approx 10$–$20\ \mu$m, inside. The vesicles are composed of a pure phospholipid and initially contain no dye, so they appear black under the fluorescence microscope (Figure 1A). The external solution contains the peptide and a green fluorescent dye, carboxyfluorescein (CF), that is highly charged and cannot permeate the vesicle membrane. When the GUVs are added to the peptide solution, the peptide permeabilizes the membrane and CF enters the outer GUV, which then exhibits bright green fluorescence (Figure 1B). The inner GUVs, however, remain black if the peptide does not cross the outer membrane (Figure 1C). But if the peptide translocates across the membrane, it will bind to, and permeabilize the inner vesicles, which will then show green fluorescence as well (Figure 1D).

Three points are worth noting. First, a peptide is considered to translocate if it crosses the membrane while the vesicle remains intact; that is, the vesicle does not burst or disintegrate in the process, but pores may open. No particular mechanism of translocation is assumed. Second, the method only works for peptides that cause at least some membrane leakage. Peptides that translocate without any leakage will not be detected. We call this “silent” translocation. Third, a variation in which the peptides are labeled with a fluorophore, also employed here, always allows detection of translocation.

Furnished with this method, we examined translocation of three amphipathic peptides, TP10W, DL-1 and CE-2, whose interactions with membranes of large unilamellar vesicles (LUVs, $d \approx 0.1\ \mu$m) we previously studied (6, 11). (See Table 1 for peptide sequences.) CE-2 is a synthetic, simplified variant of cecropin A, a moth antimicrobial peptide that we also examined before (12); DL-1 is a synthetic variant of δ-lysin, a staphylococcal cytolytic peptide we have studied extensively (13–16); and TP10W is a variant (Y3W) of the cell-penetrating peptide TP10, which we have also previously examined (5–7).

This choice of peptides was motivated by the hypothesis that the ability of membrane-active peptides to translocate across a lipid bilayer is determined by their Gibbs energy of insertion (ΔG^o_{ins}) into the membrane from the surface-associated state (17). ΔG^o_{ins} can be estimated from the difference between the Gibbs energies of binding to the membrane (ΔG^o_{bind}) and transfer from water to octanol (ΔG^o_{oct}), as a mimic of the membrane interior, calculated with the Wimley-White octanol scale (18, 19). Whereas the bilayer interior is not similar to octanol, by a fortunate coincidence ΔG^o_{oct} provides a reasonable estimate for the transfer of an α-helical polypeptide from water to the bilayer hydrophobic interior (20). The hypothesis is that if $\Delta G^o_{ins} \leq 20\,\mathrm{kcal/mol}$ the peptides translocate across the bilayer but if $\Delta G^o_{ins} \geq 23\,\mathrm{kcal/mol}$ they do not (17).

This threshold was proposed because it seemed to match a division of membrane-active peptides between those that caused graded or all-or-none release of dyes from lipid vesicles. Peptides that caused graded release had $\Delta G^o_{ins} \leq 20\,\mathrm{kcal/mol}$, whereas those that caused

all-or-none had $\Delta G^o_{ins} \geq 23\,\mathrm{kcal/mol}$ (17). TP10W (6) and DL-1 (11) belong to the graded and all-or-none classes, respectively, and conform to the above criterion. On the other hand, CE-2 has ΔG^o_{ins}=35 kcal/mol, well above the threshold, but causes graded dye release from LUVs (11). This indicates that either the hypothesis is wrong or graded release is not a reliable indicator of translocation. Recently, we have shown that, indeed, translocation cannot be inferred with certainty from graded release, because the release type can change with vesicle size (21). Here we test directly for peptide translocation with our new method.

MATERIALS AND METHODS

Chemicals

N-terminal modified peptides acetyl(Ac)-TP10W (purity 96 %), Lissamine Rhodamine B (Rh)-TP10W (97 %), Ac-DL-1a (96 %), and Rh-DL-1a (95 %) were purchased from American Peptide Company; and CE-2 (> 82 %) was purchased from Bachem. The peptide identity was ascertained by mass spectrometry, and the purity was determined by HPLC, provided by the manufacturer. Peptide stock solutions were prepared in water/ethyl alcohol 1:1 (v/v) (AAPER Alcohol and Chemical, Shel-byville, KY), stored at −80°C, and kept on ice during experiments. Peptide concentrations were determined by tryptophan (Trp) absorbance at 280 nm ($\varepsilon = 5.6 \times 10^3\ M^{-1}cm^{-1}$) or Rh absorbance at 559 nm ($\varepsilon = 8.8 \times 10^4\ M^{-1}cm^{-1}$). 1-Palmitoyl-2-oleoyl-*sn*-glycero-3-phosphocholine (POPC) and 1,2-dioleoyl-*sn*-glycero-3-phosphoethanolamine-N-lissamine rhodamine B (Rh-DOPE), in chloroform solution, were purchased from Avanti Polar Lipids (Alabaster, AL). Carboxyfluorescein (CF) and 7-methoxycoumarin-3-carboxylic acid (7MC) succinimidyl ester were purchased from Molecular Probes/Invitrogen (Carlsbad, CA). 7MC-POPE was synthesized as previously described in detail (12, 22–24). Bovine serum albumin (BSA), fatty acid-free, was purchased from ICN (Aurora, OH). Organic solvents (High performance Liquid Chromatography/American Chemical Society grade) were purchased from Burdick & Jackson (Muskegon, MI).

Confocal Fluorescence Microscopy of Giant Unilamellar Vesicles (GUVs)

POPC GUVs were prepared by electroformation (25, 26), as previous described in detail (21), except that electroformation was performed at 10 Hz for 1 h 15 min, instead of 2 h, followed by 30 min at 2 Hz. Fluorescence microscopy of GUVs was performed with an Olympus Fluoview FV1000 scanning confocal microscope, on samples prepared by adding 10 μL of GUV suspension in 0.1 M sucrose to ~ 240 μL of 0.75 μM peptide, 50 μM CF, and 0.1 M glucose, in a culture dish coated with BSA, as previously described (21). The lipid concentration is not known exactly in these experiments, but from the number and size of vesicles in the field of view, we estimate it to be ≈ 30–100 μM. Quantification of CF fluorescence emission from each vesicle was performed with ImageJ (21, 27). Initially, the vesicle interior is dark and the outside is green, from CF fluorescence, but as CF influx occurs, the fluorescence inside the vesicle increases. The degree of filling of each vesicle is given by the ratio of the fluorescence intensity inside the GUV to that outside, near the GUV of interest (21). Final images were edited for brightness and contrast with the GNU Image Manipulation Program (GIMP).

Kinetics of Peptide Binding to Large Unilamellar Vesicles (LUVs)

LUVs were prepared by extrusion through polycarbonate filters of 0.1 μm pore size (Nuclepore, Whatman, Florham, NJ), in buffer containing 20 mM MOPS, pH 7.5, 0.1 mM EGTA, 0.02 % NaN_3, and 100 mM KCl, as previously described in detail (6, 12, 13). Lipid concentrations were determined by a modified Bartlett phosphate assay (14, 28). The kinetics of peptide binding to LUVs were measured in a stopped-flow fluorimeter (SX.

18MV, Applied Photophysics), as previously described (6, 11, 12, 22). The signal monitored was the large change in fluorescence emission intensity of rhodamine (Rh) covalently attached to the peptides (Rh-TP10W and Rh-DL-1a) upon binding to the membrane, or the emission of 7MC-POPE incorporated in the bilayer (at 2 mole %), upon Förster Resonance Energy Transfer (FRET) from the intrinsic Trp residue on the peptide. Trp was excited at 280 nm, and the emission of 7MC (λ_{max} = 396 nm) was measured with a cut-off filter (GG-385, Edmund Industrial Optics, Barrington, NJ). Rhodamine was excited at 550 nm and emission was recorded through a long-pass filter (OG 590, Edmund Industrial Optics). After mixing, the concentration of peptide was 1 μM.

The binding kinetics were analyzed as previously described (12, 22). Briefly, the time traces were fitted with an exponential rising function of the form $1 - \exp(-k_{app}t)$, where t is time and k_{app} is the apparent rate constant. A plot of $k_{app} = k_{on}[Lipid] + k_{off}$, as a function of lipid concentration, [*Lipid*], yields the on-rate constant (k_{on}) from the slope and the off-rate constant (k_{off}) from the y-intercept of a linear regression. If the y-intercept occurred very close to the origin, k_{off} was obtained by measuring the dissociation kinetics directly (6, 12, 22). Briefly, the peptide was first bound to donor POPC vesicles labeled with 2 mole % 7MC-POPE, which were mixed with a large excess of unlabeled acceptor POPC vesicles in the stopped-flow instrument, using a 1:10 syringe volume ratio. The decrease observed in the FRET signal, as the peptide dissociates from the donors and associates with the acceptor vesicles, yields the kinetics of dissociation (12). Alternatively, using Rh-labeled peptides, a 1:10 dilution of the donor-bound peptide into buffer was performed in the stopped-flow instrument. The kinetics in this experiment usually contain a long-time tail, but k_{off} is well approximated by the largest rate constant, obtained by a single-exponential fit to the initial part of the curves (6, 12).

Kinetics of Peptide-Induced CF Efflux in LUVs

Carboxyfluorescein (CF) release kinetics, from LUVs containing 50 mM CF, in 20 mM MOPS buffer, pH 7.5, 0.1 mM EGTA, 0.02 % NaN_3, were measured by the relief of self-quenching of CF fluorescence inside the vesicles, in the stopped-flow fluorimeter, with excitation at 470 nm and emission recorded through a long-pass filter (OG 530, Edmund Industrial Optics), as previously described (5, 6, 11–13, 22). The fraction $F(t)$ of CF released was determined by comparison of the fluorescence with that obtained upon addition of 1 % Triton X-100, which releases all the dye from the vesicles. The kinetics of dye release were characterized quantitatively by calculating the average time constant of CF efflux (τ_E), as previously described (6, 11, 15, 16). This characteristic efflux time was obtained numerically by $\tau_E = \int tf(t)dt / \int f(t)dt$, where $f(t)$ is the time-derivative of the experimental $F(t)$ (15, 16).

RESULTS

Peptide translocation across pure phospholipid bilayers

Figure 2 shows three representative time series after addition of POPC GUVs to the peptides Rh-TP10W (A,B) and Rh-DL-1a (C). In the first image of each series, the outer vesicle is initially dark because it contains no dye (CF). In the second, the peptides have caused some CF flux into the outer vesicle. The inner vesicles are not visible in the second image because they moved out of the focal plane. Initially, the density of the solution inside the vesicles (0.1 M sucrose) is higher than outside (0.1 M glucose). Flux into the outer GUV lowers the density in its lumen, and the inner vesicles sink because of their higher density. By the third image of each series the outer vesicle has reached complete influx. The outer vesicles now appear shrunk because the microscope was focused on the bottom of these very large GUVs ($d \approx 100$ μm), where the inner vesicles gather. In Figure 2A and B, 25–75 min after GUV

addition, Rh-TP10W causes CF flux into the inner vesicles, which progressively become fluorescent. This indicates that the peptide crossed the outer membrane, associated with the membranes of the inner vesicles, and caused CF flux into them as well.

The versions of TP10W and DL-1 used in this work were labeled with the fluorophore Rhodamine-Lissamine B (Rh) at the N-terminus, to allow monitoring of binding and visualization of the membrane. Those fluorescent tags have minor effects on the peptide properties, as shown in the next section. (CE-2 was unlabeled, but 0.1 mole % of a fluorescent, headgroup-labeled rhodamine-phosphatidylethanolamine (Rh-DOPE) was included in the lipid for visualization of the membrane.) In Figure 2B, the intensity of the rhodamine fluorescence has been increased, to show Rh-TP10W on the outer and inner membranes (last two images), confirming translocation. In Figure 2C, Rh-DL-1a also causes flux into the outer vesicle. However, of 14 inner vesicles only 1 shows influx after 70 minutes. Thus, both peptides are able to translocate but Rh-TP10W appears to do so more efficiently than Rh-DL-1a.

Figure 3 shows a GUV containing several inner vesicles, 44 minutes after addition to a solution of Rh-TP10W. Figure 3A shows the CF fluorescence (water-soluble dye) and the Rh fluorescence (Rh-labeled peptide). Figure 3B shows the Rh channel only. In this experiment, the intensity of the Rh channel was enhanced to allow observation of the weaker fluorescence in the membrane of the inner vesicles. In Figure 3A, the outer vesicle has already undergone complete influx at ~ 20 min after addition to the peptide. Five of the inner vesicles are large (≥10 μm = scale bar); of those five, the inner vesicle on the bottom right is undergoing influx, indicating that Rh-TP10W translocated across the outer membrane. This is even more evident in Figure 3B, which shows only the Rh-labeled peptide on the membranes. What these data also show is that the peptide may reside on the inner membranes for a long time without causing influx, as happens in the other four inner vesicles.

We measured the fluorescence intensity as a function of time on the membrane of the inner vesicle that undergoes influx in Figure 3A, as well as the influx into its lumen. Figure 3C shows the fluorescence intensity on the membrane of the inner vesicle (red points) relative to the outer vesicle. The kinetics depicted by the red line represent the function $1 - \exp(-t/\tau_R)$, where $\tau_R \approx 6$ min, which describe the data well. This increase in fluorescence on the inner membranes represents only *apparent* binding. We know from binding and dissociation kinetics measured by stopped-flow in LUVs (see below) that the real binding is very fast, occurring in ~ 0.1 sec under these conditions ($k_{on} = 2.3 \times 10^4\ M^{-1}s^{-1}$ and lipid concentration inside the outer vesicle ~ 1 mM). Similarly, dissociation from the inner side of the outer membrane occurs in a few seconds ($k_{off} = 0.4\ s^{-1}$). The time course of the appearance of Rh-TP10W on the inner membrane must therefore reflect a much slower process, which is rate-limiting. That process can only be translocation across the outer membrane. The characteristic time measured on 11 vesicles in 4 independent preparations was $\langle\ \tau_R\ \rangle = 10 \pm 6$ min (mean ± SD).

The flux into the inner vesicle is shown by the green data points in Figure 3C, quantified by the fluorescence intensity inside that vesicle relative to the outside. It occurs over the same time period as peptide translocation across the outer membrane, but with very different kinetics. While translocation follows approximately an exponential rise, influx occurs almost abruptly, ~ 10 min after the peptide begins to accumulate on the inner membrane. Further, the degree of filling only reaches ~ 50 % in this vesicle.

Figure 4 shows equivalent plots in two other GUVs, in which the flux into the outer vesicle was also recorded (blue data points). In Figure 4A influx reaches ~ 100 % in both the outer

and inner vesicles, and the jump is very abrupt in the inner one (green). Usually, flux into the outer vesicle is slightly slower than in the inner ones, but in this particular GUV it is slower than in most (see Figure 7 for additional examples). Occasionally, influx into the inner vesicle is more continuous or displays only little jumps (Figure 4B). But vesicles with large influx jumps are by far the most common. In all cases, most of the translocation across the outer membrane (red) occurs *after* influx into the outer vesicle (blue).

What was unexpected was the result of the experiment shown in Figure 5. We asked the question of whether some peptides translocate across the outer membrane *before* causing influx in that same outer vesicle. Figure 5A shows a GUV in both the CF channel (water-soluble dye, green) and the Rh channel (peptide fluorescence, red), 74 min after addition to Rh-TP10W. The inside of the outer vesicle is black, indicating there is no influx at this point. Yet a faint rhodamine fluorescence is discernible on the membrane of the inner vesicles. In Figure 5B only the Rh channel is shown, with strongly increased contrast to reveal the peptide fluorescence on the membranes. Clearly, Rh-TP10W is present on the inner vesicles. It translocated across the outer membrane but has not caused CF flux into the outer vesicle. The fluorescence on the inner vesicles is faint, indicating that the number of peptides that translocated is small. But they have translocated "silently," without significantly perturbing the outer membrane.

Thermodynamics of binding and efflux rates in LUVs

We were concerned with the possibility that the N-terminal rhodamine modification of the peptides would alter their membrane binding affinity or the rate of dye flux they induce in lipid vesicles. Therefore, the equilibrium constants for dissociation (K_D) from the membrane and the characteristic efflux times (τ_E) were measured in large unilamellar vesicles (LUVs, $d \approx 0.1\ \mu$m) and compared with those of unlabeled peptides. The K_D were determined by measuring the rate constants for binding (k_{on}) and dissociation (k_{off}) of the peptides in LUVs by stopped-flow fluorescence, as we have done extensively for a number of membrane-active peptides (5, 6, 11, 12, 17). The binding kinetics were monitored by the change in FRET from an intrinsic Trp residue on the peptide to a lipid fluorophore (7MC-POPE) incorporated in the bilayer, or by the change in fluorescence intensity of the rhodamine upon binding of Rh-labeled peptides to the membrane as a function of time. Measuring the apparent rate constants (k_{app}) that characterize the binding kinetics as function of the lipid concentration yields the on- and off-rate constants from $k_{app} = k_{on}[Lipid]+k_{off}$. Figure 6 shows examples of kinetic binding curves and plots of k_{app} as a function of lipid concentration for each peptide.

In the case of Ac-TP10W, there was sufficient uncertainty in the y-intercept (Figure 6C) that we determined k_{off} by measuring the dissociation kinetics directly (6, 12, 22). The peptide was first bound to donor POPC LUVs labeled with 2 mole % 7MC-POPE, which were then mixed with a large excess of unlabeled acceptor POPC LUVs in the stopped-flow instrument, using a 1:10 syringe volume ratio. As the peptide dissociates from the donors (labeled) and associates with the acceptor vesicles (excess, unlabeled), the FRET signal decreases. The dissociation kinetics recorded were well approximated by the largest rate constant of the decay, obtained by a single-exponential fit to the initial part of the curves. The value listed in Table 1 for Ac-TP10W was obtained by this method, which is in good agreement with the y-intercept obtained from the association kinetics shown in Figure 6C.

The equilibrium dissociation constant was calculated from $K_D = k_{off}/k_{on}$. The Gibbs free energy of binding is then obtained by $\Delta G^{o}_{bind} = \ln K_D - 2.4\ \mathrm{kcal/mol}$, where the last term switches from molar to mole fraction units (19). This transformation is performed to compare these experimental values with those calculated with the Wimley-White interfacial

binding scale (19, 29). Table 1 shows the values of the Gibbs free energies of binding (ΔG^o_{bind}) and transfer from water to octanol (ΔG^o_{oct}), and their difference, the Gibbs energy of insertion ($\Delta G^o_{ins}=\Delta G^o_{oct}-\Delta G^o_{bind}$). The values of k_{on} and k_{off} used to calculate K_D are also listed.

The effects of peptide terminal modifications were estimated from experiment and by the Wimley-White interfacial and octanol scales (18, 19, 29–31, 33). Judging from the differences observed between N-terminal variants of TP10W and DL-1a (Table 1), binding of Rh-labeled peptides is less favorable than binding of acetylated (Ac) peptides by $\Delta\Delta G^o_{bind} \approx +0.5\,\mathrm{kcal/mol}$. But binding of acetylated peptides is more favorable than binding of the original peptides by $\Delta\Delta G^o_{bind} \approx -1.5\,\mathrm{kcal/mol}$. Thus, Rh-labeled peptides bind to POPC membranes with a ΔG^o_{bind} that is intermediate between those of the original and acetylated peptides (Table 1). Therefore, we assume ΔG^o_{oct} of Rh-labeled peptides to be also intermediate. The uncertainty in ΔG^o_{oct} of Rh-TP10W and Rh-DL-1a is estimated to be ~ ±1 kcal/mol, which is small compared to their values ($\Delta G^o_{oct}=8$and 16 kcal/mol, respectively). In conclusion, the changes in binding and transfer to octanol imparted by the attachment of the rhodamine to the N-terminus of the peptides are small and unlikely to cause a significantly different behavior compared to the original peptides, and especially compared to the acetylated variants. Since the changes in ΔG^o_{ins} are minor, the predictions of the hypothesis regarding the ability to translocate should hold for the modified peptides, possibly with the exception of Ac-DL-1a, which falls just short of the threshold proposed for non-translocating peptides.

To assess the effect of terminal modifications on peptide activity, we also measured efflux rates of CF from LUVs upon peptide addition, by stopped-flow fluorescence, as described extensively before (5, 6, 11–13, 22). Briefly, CF is self-quenched when it is encapsulated at high concentrations in the vesicles, but its fluorescence increases dramatically as it is released to the outside and self-quenching is relieved. To quantify the peptide activity in a model-free way, we calculated the average time constant of dye efflux (τ_E) numerically by $\tau_E = \int tf(t)dt/\int f(t)dt$, where $f(t)$ is the time-derivative of the fraction of CF released as a function of time (15, 16). The values of τ_E obtained at 50 μM lipid and 1 μM peptide are listed in Table 1. The τ_E of the modified peptides vary only by factors of ~ 2–3 compared to the original ones. Thus, the peptide terminal modifications do not result in large changes in activity.

Distributions of influx times in GUVs

It is clear that all peptides tested are able to translocate across the membrane of GUVs, but they do so to different extents or at different rates. The question is whether the rate of influx into the inner vesicles is different from that in the outer GUV. If only a small fraction of peptides were to translocate, and if binding of many to the membrane of the inner vesicles were necessary to induce influx, the time required for influx could be much longer than in the outer vesicle. Figure 7 shows examples of time traces of CF flux into inner GUVs (black lines) compared with influx into the outer GUV (red) for the three peptides examined, (A) Rh-TP10W, (B) Rh-DL-1a, and (C) CE-2.

To answer the question, we compared the half-time of flux into the inner vesicles (τ_i) relative to that of the outer vesicle (τ_o). The half-time is defined as the mid-point of the sharp increase in degree of filling apparent in the curves of Figure 7. Because different samples have significant fluctuations in lipid concentrations, and the bound peptide-to-lipid ratio determines to a large extent the rate of flux of dyes across the membrane (34), τ_i for the inner vesicles are expressed relative to τ_o. The density of τ_i was calculated by dividing the number of inner vesicles with τ_i in each interval [$n\ \tau_o$, $(n + 1)\ \tau_o$] (n = 1, 2..) by the number

of inner vesicles monitored for a time $t \geq (n+1)\ \tau_o$. The density distributions obtained are shown in Figure 8, as functions of the bin number n, in units of τ_o.

Most inner vesicles observed for very long times, $t \sim 10–20\ \tau_o$, eventually showed influx. However, most vesicles were not (and cannot be) observed for such long times, and the significance of those observations is unclear because the GUVs are not stable in the presence of peptide in the long run. Therefore, the distributions shown in Figure 8 were truncated at $6\,\tau_o$. Beyond that time, the data is too sparse to calculate a meaningful density. A summary of all the data is shown in Table 2.

The distributions in Figure 8 show that in the presence of Rh-TP10W or Rh-DL-1a the influx times τ_i of the inner vesicles are comparable to those of the outer vesicles, τ_o. The weighted averages are $\langle \tau_i \rangle = 2.7\ \tau_o$ for Rh-TP10W and $\langle \tau_i \rangle = 2.4\ \tau_o$ for Rh-DL-1a. For CE-2 the data is too sparse, but we include the plot in Figure 8 for the sake of completeness and symmetry. Note, however, that τ_i is the time from the beginning of the experiment. The influx time *after* influx of the outer vesicle is $\langle \tau_i \rangle - 1$, which is $1.7\ \tau_o$ for Rh-TP10W and $1.4\ \tau_o$ for Rh-DL-1a. Thus, peptides that translocate cause flux into the inner vesicles in similar time as in the outer ones.

DISCUSSION

Methods to assess peptide translocation

Assessing peptide translocation has often relied on fluorescence-quenching assays based on the interaction between peptides and fluorophores incorporated in the membrane of large unilamellar vesicles (LUVs), or on fluorescence inactivation by the water-soluble reducing agent dithionite, whose access to the interior of LUVs is enabled by peptide translocation (35, 36). However, these methods are prone to artifacts, because of lipid flip-flop, photobleaching, or dithionite diffusion into the vesicle interior.

A second approach is to encapsulate in LUVs a proteolytic enzyme, which hydrolyzes the peptides that translocate, or to add the enzyme to the outside and measure peptide protection from hydrolysis if translocation occurs (35–37). These methods, too, suffer from several complications. First, the signal that indicates translocation is usually a small difference in a fluorescence amplitude. Second, if protection is measured, it is difficult to convincingly distinguish translocation from mere insertion into the bilayer. Third, movement of trypsin itself across the bilayer remains a concern. Finally, trypsin is prone to self-hydrolysis as a consequence of the vesicle encapsulation procedure.

Other approaches to assess peptide translocation (5, 14, 38) are based on kinetics of interactions of peptides with LUVs measured by time-resolved fluorescence (including stopped-flow), which we have used extensively. These methods, however, are very indirect. Translocation is inferred as a necessary step to fit the kinetics, but is not directly observed, though the present experiments are consistent with those inferences (5, 13, 14).

More recently, two improvements were reported. One uses a special modification of the peptides (39), but the second is quite general (40). The protease chymotrypsin (which seems to work better than trypsin) is encapsulated in LUVs, and translocation is measured by the rate of proteolytic cleavage of the peptide that enters the vesicles. If the protease leaks out, however, the rate of peptide hydrolysis will decrease and the kinetics of peptide translocation will appear slower than they are. The assay depends on the presence of a chymotrypsin cleavage site in the peptide sequence (an aromatic residue) but this is a feature of most antimicrobial and cell-penetrating amphipathic peptides.

GUVs have also been used in combination with fluorescently-labeled peptides to assess translocation, but the signals from the peptide were weak in earlier work (41). More recently, multilayered GUVs and multilamellar vesicles (MLVs) were used to assess translocation by the appearance of fluorescently-labeled peptides on interior bilayers (40, 42), but reliance on peptide labeling with fluorophores remains a restriction on these methods. In addition, interior bilayers in those vesicles seem to lie sufficiently close to the outer membrane for direct peptide movement from one bilayer to an adjacent one to be a concern. In the experiments described here, we were particularly careful in selecting outer vesicles containing truly independent inner vesicles, not invaginations of the outer membrane, or multilayered vesicles. On the other hand, He et al. (40) used MLVs to measure a translocation half-time of 3–5 min for the Rh-labeled peptide S4 (a 20-residue amphipathic sequence of a voltage-gated potassium channel), which is entirely consistent with $\langle \tau_R \rangle = 10 \pm 6$ min measured here for translocation of Rh-TP10W across the outer membrane of a GUV. Thus, the measurements in MLVs seem to yield similar results to those obtained here on GUVs with inner vesicles.

Advantages and limitations of the present method

Our method has several advantages but also has limitations that should be noted. First, relying solely on influx of an external dye into the lumen of inner vesicles contained inside larger GUVs, it can be used to determine translocation of any peptide, independent of whether it contains a proteolytic cleavage site or a fluorescent label. Its main limitation is that it cannot be used if peptides translocate silently, that is, without causing dye flux. Some peptides are known to behave in this fashion (43, 44). On the other hand, Rh-TP10W, which also translocates silently at first (Figure 5), later causes influx. Thus, it is possible that other silent peptides eventually (or at higher concentrations) cause dye influx, rendering them sensitive to the method. We plan to examine this question in the future.

Second, the method answers the question of whether peptides translocate or not, but again, if it relies solely on observation of influx, it does not exactly yield the kinetics of translocation. The kinetics of translocation are different from those of influx (Figures 3C and 4). This problem can be surmounted by using rhodamine-labeled peptides, which behave similarly to acetylated peptides in terms of binding and induced flux (Table 1). As shown here, this becomes a source of important information, because the time courses of translocation and influx are obtained simultaneously and independently.

A third limitation is the time consumed collecting statistically significant numbers of observations in inner vesicles, because there are not many GUVs with inner vesicles in any given preparation. However, we found that reducing the time of electroformation at 10 Hz from 2 h to 1 h 15 min significantly increases the number of GUVs with inner vesicles. The longer electroformation times probably disrupt the very large GUVs that contain inner ones.

Consequences for the mechanism of membrane-active peptides

Finally, we consider the consequences of the experimental results for our understanding of the mechanisms of interaction of amphipathic peptides with membranes. Using rhodamine-labeled peptides, we measured the kinetics of peptide movement across the membrane of a GUV, from the time-course of appearance of peptide fluorescence on the membrane of vesicles inside that GUV (Figures 3C and 4, red data). Simultaneously, we measured dye flux into the outer and inner vesicles (blue and green data, respectively). Translocation and influx are thus compared directly in the same GUV. In the case of Rh-TP10W, the kinetics of the two processes are very different. Translocation across the outer membrane is a gradual, approximately exponential increase. In contrast, dye flux is usually an abrupt event (Figure 7 shows more examples). The bulk of dye flux into the *outer* GUV happens before,

or at the very beginning of peptide translocation across its membrane. Flux into the *inner vesicles* occurs sometime during peptide translocation across the outer membrane, but its exact moment is unpredictable. Incidentally, the sharpness of the influx events and their stochastic occurrence indicates that the characteristic time of flux observed in macroscopic samples of LUVs represents the average time it takes to form a pore, not the time of dye flux through the pore (17).

Evidently, peptide translocation and dye flux are not concomitant events. This is confirmed by the appearance of fluorescent peptides on the inner vesicles of a GUV whose membrane remains tight to dye influx (Figure 5). Thus, a little translocation happens *before* any dye influx occurs. Mechanistic coupling of flux and translocation has been assumed by most investigators, including ourselves in the analysis of dye efflux in LUVs, but the present results show that some of those conclusions may need revision.

Membrane permeabilization appears to be the result of peptide-induced stochastic fluctuations in lipid organization in the bilayer. Some of those fluctuations are large enough for a pore to open and influx to occur. These features are consistent with a chaotic pore (12, 45), not with a peptide-lined channel. It should be noted also that the vesicles remain intact during permeabilization; that is, they do not burst or disintegrate in the presence of the peptide (at the low concentrations used here). And peptides may reside on a GUV membrane for a long time without causing influx.

Influx jumps are often intuitively associated with all-or-none flux, whereas a slow leakage of dye across the membrane would be expected for graded flux. Jumps of influx to ~ 100 % are often observed, though in some vesicles the jump is to ~ 50 % or less (Figures 3C, 4, and 7). These abrupt jumps occur even with peptides, such as CE-2 and TP10 (Rh-TP10W), that cause graded dye flux in lipid vesicles (LUVs and small GUVs) (5, 11, 21). Though not necessarily intuitive, these results agree with our previous conclusion that the nature of graded and all-or-none fluxes is statistical, not kinetic (21). That is, graded or all-or-none fluxes reflect the distribution of the vesicle population as a function of dye content, not the rate of individual leakage events. This distribution may be bimodal, consisting mainly of vesicles either empty or full (all-or-none flux), or it may be unimodal, centered on ~ 50 % filling (graded flux). But the individual flux events are almost always abrupt, just not always complete (Figures 3C, 4, and 7). Thus, observation of graded or all-or-none behavior may provide hints but no definite conclusions on the molecular mechanisms of membrane permeabilization by these peptides.

We have noted that Rh-TP10W can cross the vesicle membrane to some extent *before* causing any dye influx. We have called this “silent” translocation. Our experiments do not rule out that translocation may also occur when pores form, but its silent occurrence indicates that translocation does not necessarily take place only in the pore regions. Rather, it suggests that another path for translocation exists, in which the peptide penetrates the bilayer with little perturbation, perhaps as a monomer, as suggested for TP10 (5).

At present, it appears to us that peptide translocation and dye flux across a lipid bilayer occur broadly over the same period, but in parallel, without a mandatory mechanistic connection. The Gibbs energy of peptide insertion into the lipid bilayer from the surface-associated state (ΔG^o_{ins}) may determine both translocation and flux. There are significant correlations between the rate of flux and ΔG^o_{bind} or ΔG^o_{oct}, the components of ΔG^o_{ins} (6, 11). Almeida and Pokorny (17) proposed the hypothesis that the ability of peptides to translocate across the membrane is determined by ΔG^o_{ins}. We now found that the three peptides examined can translocate, but with different probabilities, which decrease as ΔG^o_{ins} increases. Rh-TP10W has $\Delta G^o_{ins}{=}17\,\mathrm{kcal/mol}$ and caused influx in 53 % of the inner

vesicles; Rh-DL-1a has $\Delta G^{o}_{ins} \sim 24\,\mathrm{kcal/mol}$ and caused influx in 25 %; and CE-2 has $\Delta G^{o}_{ins} = 35\,\mathrm{kcal/mol}$ and caused influx in only 2 % of the inner vesicles (Table 2). These results are consistent with the hypothesis in a probabilistic sense.

Acknowledgments

This work was supported by grant GM072507 from the National Institutes of Health. We thank Dr. Richard Dillaman and Mark Gay for the use of the confocal fluorescence microscope, a facility funded by National Science Foundation grant DBI 0420948.

References

1. Langel, U. Handbook of Cell Penetrating Peptides. 2. CRC Press; Boca Raton, FL: 2006.
2. Derossi D, Calvet S, Trembleau A, Brunissen A, Chassaing G, Prochiantz A. J Biol Chem. 1996; 271:18188–18193. [PubMed: 8663410]
3. Green M, Weston PM. Cell. 1988; 55:1179–1188. [PubMed: 2849509]
4. Frankel AD, Pabo CO. Cell. 1988; 55:1189–1193. [PubMed: 2849510]
5. Yandek LE, Pokorny A, Floren A, Knoelke K, Langel U, Almeida PFF. Biophys J. 2007; 92:2434–2444. [PubMed: 17218466]
6. McKeown AN, Naro JL, Huskins LJ, Almeida PF. Biochemistry. 2011; 50:654–662. [PubMed: 21166473]
7. Yandek LE, Pokorny A, Almeida PFF. Biochemistry. 2008; 47:3051–3060. [PubMed: 18260641]
8. Sakai N, Matile S. J Am Chem Soc. 2003; 125:14348–14356. [PubMed: 14624583]
9. Rothbard JB, Jessop TC, Lewis RS, Murray BA, Wender PA. J Am Chem Soc. 2004; 126:9506–9507. [PubMed: 15291531]
10. Menger FM, Sredyuk VA, Kitaeva MV, Yaroslavov AA, Melik-Nubarov NS. J Am Chem Soc. 2003; 125:2846–2847. [PubMed: 12617630]
11. Clark KS, Svetlovics J, McKeown AN, Huskins L, Almeida PF. Biochemistry. 2011; 50:7919–7932. [PubMed: 21870782]
12. Gregory SM, Cavenaugh AC, Journigan V, Pokorny A, Almeida PFF. Biophys J. 2008; 94:1667–1680. [PubMed: 17921201]
13. Pokorny A, Almeida PFF. Biochemistry. 2004; 43:8846–8857. [PubMed: 15236593]
14. Pokorny A, Birkbeck TH, Almeida PFF. Biochemistry. 2002; 41:11044–11056. [PubMed: 12206677]
15. Pokorny A, Almeida PFF. Biochemistry. 2005; 44:9538–9544. [PubMed: 15996108]
16. Pokorny A, Yandek LE, Elegbede AI, Hinderliter A, Almeida PFF. Biophys J. 2006; 91:2184–2197. [PubMed: 16798807]
17. Almeida PF, Pokorny A. Biochemistry. 2009; 48:8083–8093. [PubMed: 19655791]
18. Wimley WC, Creamer TP, White SH. Biochemistry. 1996; 35:5109–5124. [PubMed: 8611495]
19. White SH, Wimley WC. Annu Rev Biophys Biomol Struct. 1999; 28:319–365. [PubMed: 10410805]
20. Jayasinghe S, Hristova K, White SH. J Mol Biol. 2001; 312:927–934. [PubMed: 11580239]
21. Wheaten SA, Lakshmanan A, Almeida PF. Biophys J. 2013; 105:432–443. [PubMed: 23870264]
22. Almeida PF, Pokorny A. Methods Mol Biol. 2010; 618:155–169. [PubMed: 20094864]
23. Frazier ML, Wright JR, Pokorny A, Almeida PFF. Biophys J. 2007; 92:2422–2433. [PubMed: 17218467]
24. Vaz WLC, Hallmann D. FEBS Lett. 1983; 152:287–290.
25. Angelova MI, Soléau S, Méléard P, Faucon JF, Bothorel P. Prog Colloid Polym Sci. 1992; 89:127–131.
26. Apellániz B, Nieva JL, Schwille P, García-Sáez AJ. Biophys J. 2010; 99:3619–3628. [PubMed: 21112286]
27. Collins TJ. BioTechniques. 2007; 43:25–30. [PubMed: 17936939]

28. Bartlett GR. J Biol Chem. 1959; 234:466–468. [PubMed: 13641241]
29. Wimley WC, White SH. Nat Struct Biol. 1996; 3:842–848. [PubMed: 8836100]
30. Hristova K, White SH. Biochemistry. 2005; 44:12614–12619. [PubMed: 16156674]
31. Almeida PF. Methods Mol Biol. 2011; 683:81–98. [PubMed: 21053124]
32. Snider C, Jayasinghe S, Hristova K, White SH. Protein Sci. 2009; 18:2624–2628. [PubMed: 19785006]
33. Jaysinghe, S.; Hristova, K.; Wimley, W.; Snider, C.; White, SH. Membrane Protein Explorer. 2013. http://blanco.biomol.uci.edu/MPEx
34. Tamba Y, Yamazaki M. J Phys Chem B. 2009; 113:4846–4852. [PubMed: 19267489]
35. Matsuzaki K, Murase O, Fujii N, Miyaijima K. Biochemistry. 1995; 34:6521–6526. [PubMed: 7538786]
36. Matsuzaki K, Yoneyama S, Murase O, Miyaijima K. Biochemistry. 1996; 35:8450–8456. [PubMed: 8679603]
37. Kobayashi S, Chikushi A, Tougu S, Imura Y, Nishida M, Yano Y, Matsuzaki K. Biochemistry. 2004; 43:15610–15616. [PubMed: 15581374]
38. Keller S, Bothe M, Bienert M, Dathe M, Blume A. ChemBioChem. 2007; 8:546–552. [PubMed: 17330902]
39. Marks JR, Placone J, Hristova K, Wimley WC. J Am Chem Soc. 2011; 133:8995–9004. [PubMed: 21545169]
40. He J, Hristova K, Wimley W. Angew Chem Int Ed. 2012; 51:7150–7153.
41. Barany-Wallje E, Keller S, Serowy S, Geibel S, Pohl P, Bienert M, Dathe M. Biophys J. 2005; 89:2513–2521. [PubMed: 16040762]
42. Rodrigues M, Santos A, de la Torre BG, Radis-Baptista G, Andreu D, Santos NC. Biochim Biophys Acta. 2012; 1818:2707–2717. [PubMed: 22749950]
43. Krauson AJ, He J, Wimley WC. J Am Chem Soc. 2012; 134:12732–12741. [PubMed: 22731650]
44. Cruz J, Mihailescu M, Wiedman G, Herman K, Searson PC, Wimley WC, Hristova K. Biophys J. 2013; 104:2419–2428. [PubMed: 23746514]
45. Axelsen PH. Biophys J. 2008; 94:1549–1550. [PubMed: 18065456]

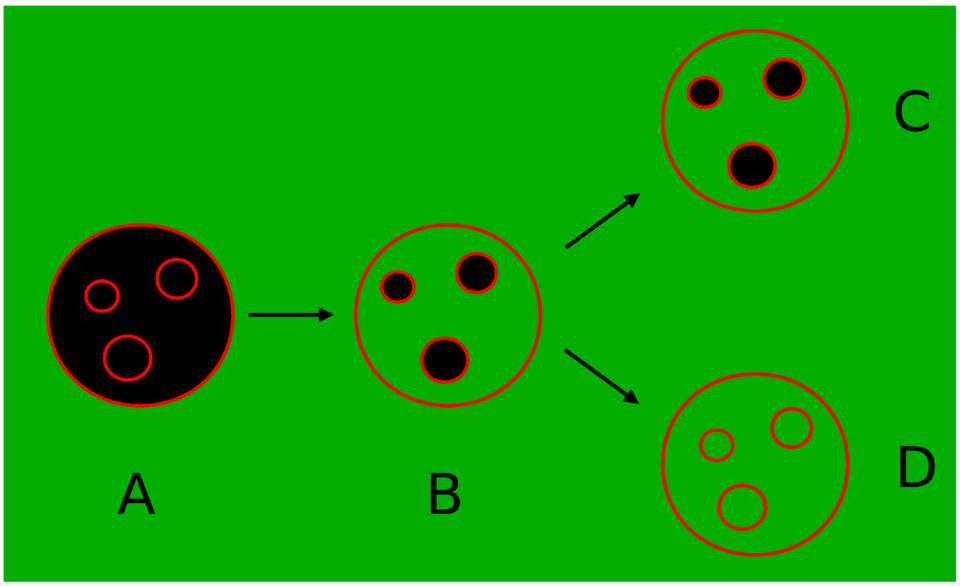

Figure 1.
The concept of the experiment. GUVs prepared with inner vesicles are added to a solution containing peptide and a water-soluble fluorophore (green). The membrane of the vesicles is shown in red. Initially (A), the interior of the vesicles has no fluorescence (black). In (B) the peptide induced flux into the outer vesicle. If the peptide does not translocate across the outer membrane, the inner vesicles remain dark (C). Appearance of fluorescence inside inner vesicles indicates that the peptide translocated across the membrane of the outer vesicle (D).

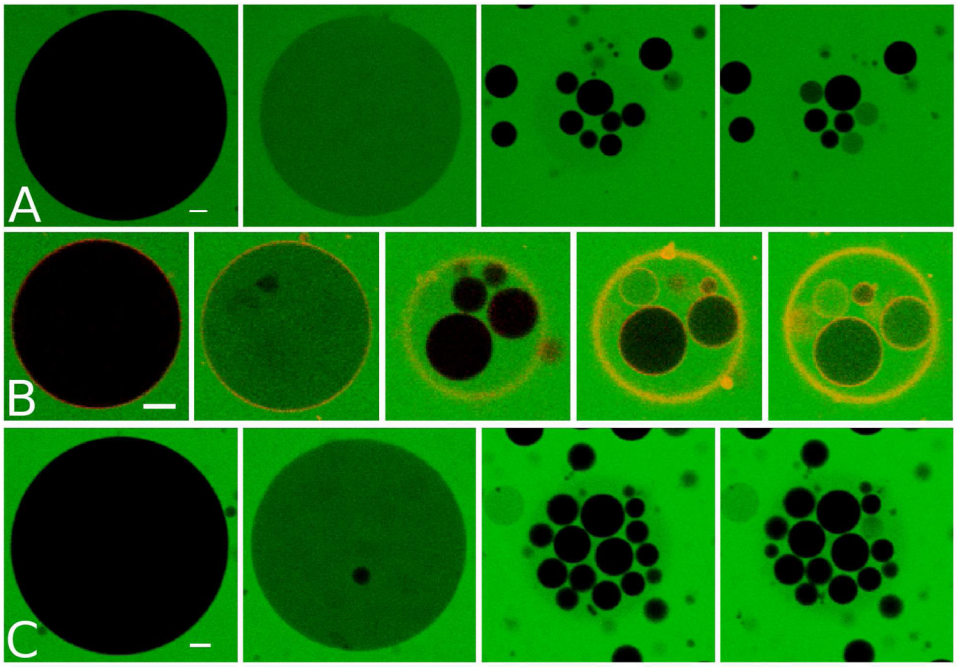

Figure 2.

Sequences of CF (green fluorescence) influx into POPC GUVs as a function of time upon addition to a solution of (A and B) Rh-TP10W or (C) Rh-DL-1a. In (B) the amplification of the rhodamine channel was increased to show the rhodamine labeled peptide on the membrane of the inner vesicles (last images of the series). The times of each frame, from the moment of addition of the GUVs to the peptide are (A) 11.5, 21.5, 25, and 29 min; (B) 8.5, 14, 33, 60, and 75 min; (C) 14, 19, 27, and 28–69 min. Peptide concentration = 0.75 μM, lipid concentration ~ 50 μM. Scale bar, 10 μm.

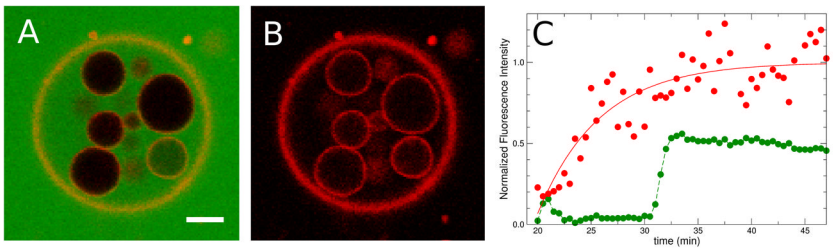

Figure 3.

Large GUV with inner vesicles 44 min after addition of the peptide Rh-TP10W. (A) CF and Rh channels. (B) Rh channel only. Scale bar, 10 μm. (C) Fluorescence of the inner vesicle at the bottom right in A and B, as a function of time. Red points, Rh channel, showing Rh-TP10W on the inner vesicle membrane. Green points, CF channel, showing flux into the inner vesicle (intensity relative to the outer membrane). The red line is $1 - \exp[-(t - t_o)/\tau_R]$ where $\tau_R = 5.8$ min and $t_o \approx 20$ min (beginning of recording). The green line is only to guide the eye.

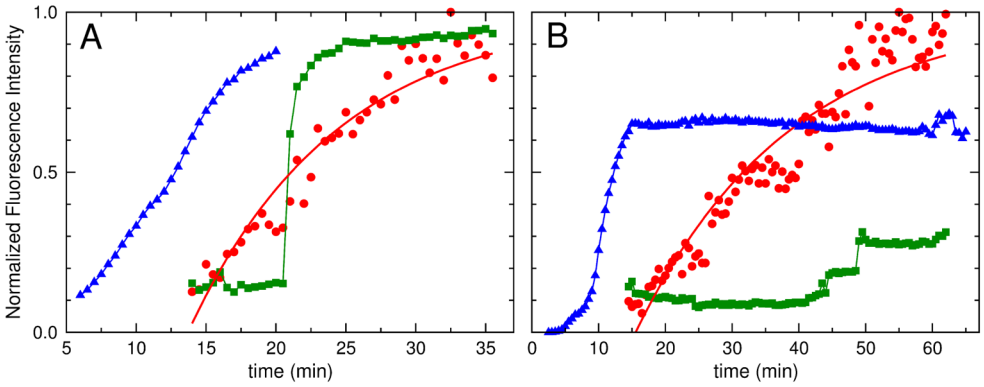

Figure 4.

Flux and translocation as a function of time in two different vesicles (A,B) upon addition to Rh-TP10W. Data and fits as in Fig. 3. Red, translocation across the outer vesicle membrane. Green, dye flux into the inner vesicle. Blue, dye flux into the outer GUV. Fits (red lines) yield (A) τ_R = 6.6 min and (B) τ_R = 23 min. Vesicle (B) moved out of the focal plane at the end of the period shown.

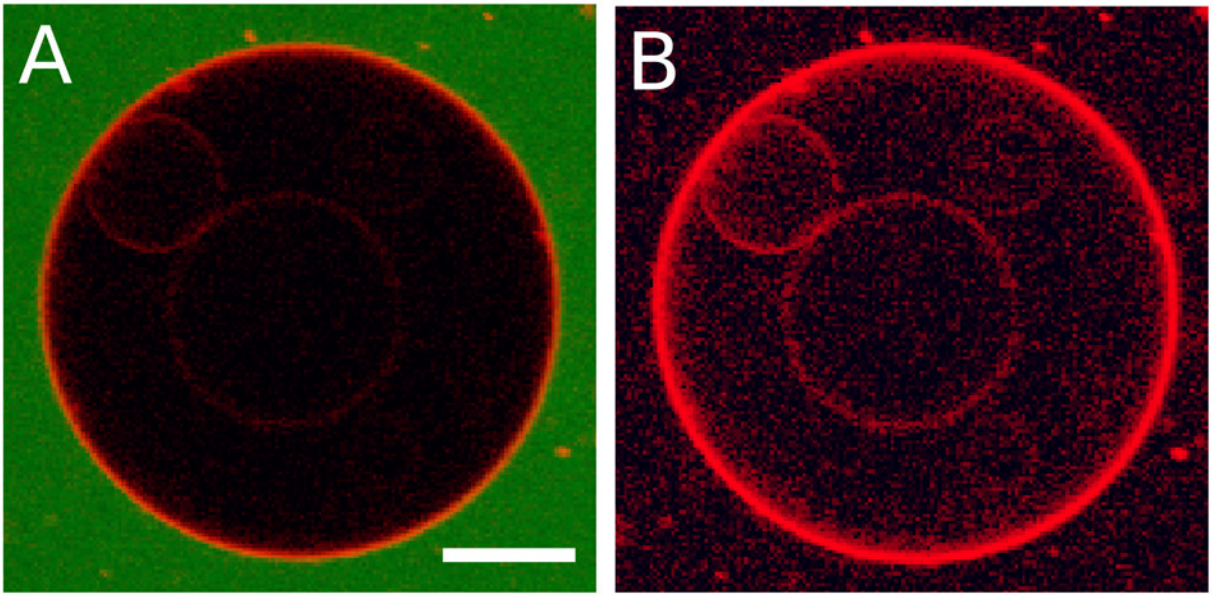

Figure 5.
Vesicle at 74 min from beginning of experiment showing inner vesicles with Rh-TP10W on their membranes (A) CF and Rh channels. No CF influx into the outer vesicle was observed. (B) Rh channel, enhanced, showing inner vesicles with Rh-TP10W. Scale bar, 20 μm.

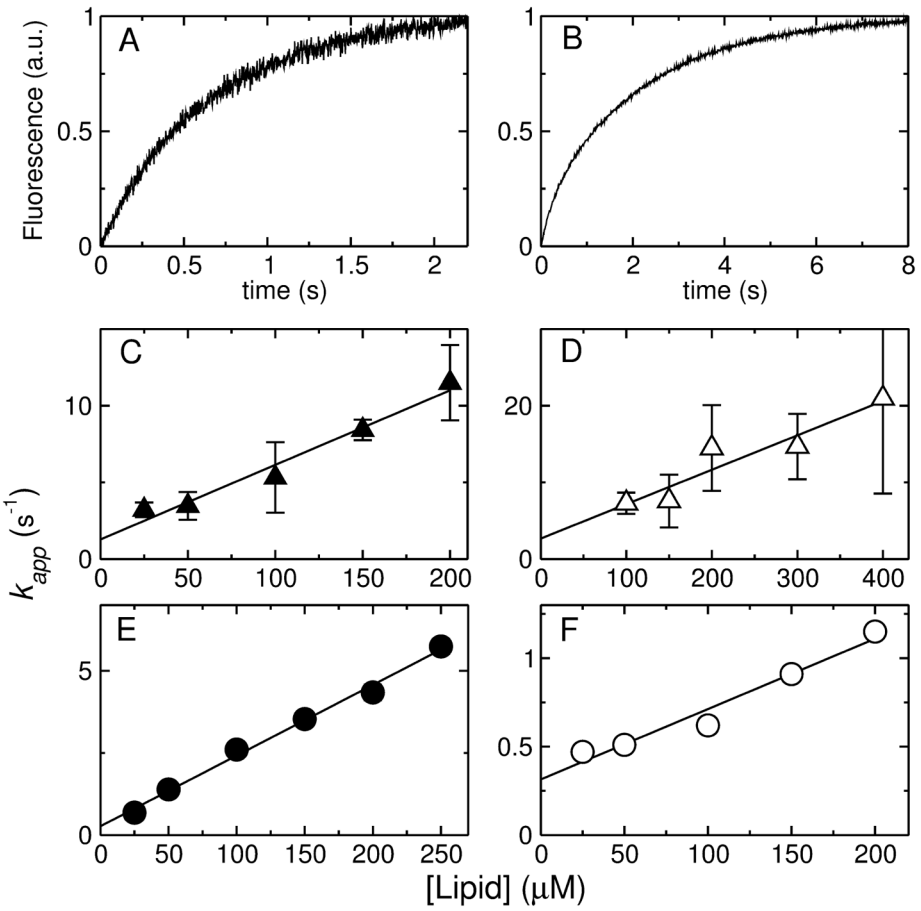

Figure 6.

Examples of binding kinetics curves for (A) Rh-TP10W and (B) Rh-DL-1a, with 1 μM peptide and 50 μM lipid concentrations, and plots of k_{app} as a function of lipid concentration for (C) Ac-TP10W, (D) Ac-DL-1a, (E) Rh-TP10W, and (F) Rh-DL-1a. In (E) and (F) the error bars are inside the points.

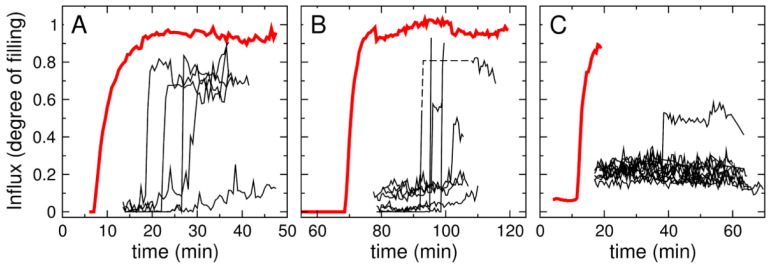

Figure 7.

Time traces of CF flux into inner GUVs (black) compared with the influx into the outer GUV (red). (A) Rh-TP10W, (B) Rh-DL-1, and (C) CE-2. The fluorescence intensity inside the vesicles is measured relative to an area outside the vesicles. The dashed line in (B) traces a vesicle whose track was temporarily lost, as it drifted out of focus.

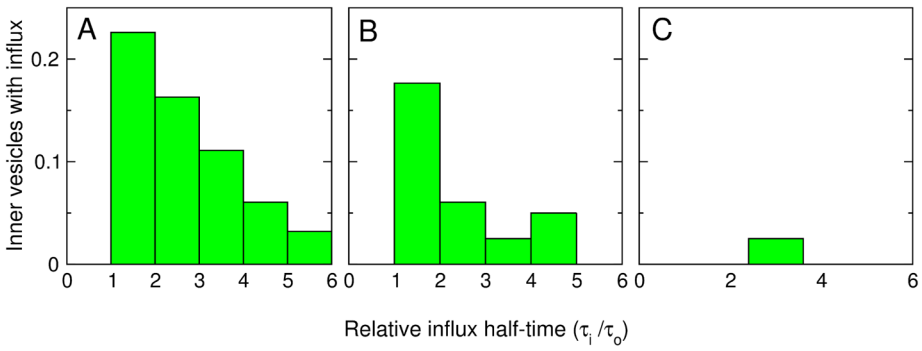

Figure 8.

Density distributions of influx half-times of the inner vesicles for (A) Rh-TP10W, (B) Rh-DL-1a, and (C) CE-2. The times of the midpoints in the influx curves (Figure 7) of the inner vesicles (τ_i) are expressed relative to their outer vesicle (τ_o) in each sample, and all inner vesicles are pooled for each peptide.

Table 1

Gibbs energies of transfer (in kcal/mol) and efflux times in LUVs for the peptides TP10W, DL-1, CE-2, and their variants.

Peptide	ΔG^o_{bind}[a]	ΔG^o_{oct}[b]	ΔG^o_{ins}[c]	k_{on} ($M^{-1}s^{-1}$)	k_{off} (s^{-1})	τ_E (sec)[d]
TP10W[e]	−7.7	9.3	17	9.4×10^4	13	12
Ac-TP10W[f]	−9.5	7.0	17	8.3×10^4	0.5	6.3
Rh-TP10W	−8.9	~ 8	~ 17	2.3×10^4	0.4	8.0
DL-1[g]	−7.0	19	26	2.5×10^4	10	4.9
Ac-DL-1a[h]	−8.3	14	22	3.1×10^4	1.4	8.7
Rh-DL-1a	−7.9	~ 16	~ 24	3.8×10^3	0.37	1.7
CE-2[i]	−5.6	30	35	3.0×10^4	140	~ 2×10^4

[a] Calculated from the experimentally determined dissociation constant by $\Delta G^o_{bind} = \ln K_D - 2.4\,\mathrm{kcal/mol}$, where the last term switches from molar to mole fraction units(19). The experimental error (SD) in these measurements is ±0.1 to 0.4 kcal/mol, except for Ac-DL-1a, where it is ±0.6 kcal/mol.

[b] Calculated with the Wimley-White octanol scale (18, 19) using Membrane Protein Explorer (MPEx)(32, 33).

[c] $\Delta G^o_{ins} = \Delta G^o_{oct} - \Delta G^o_{bind}$.

[d] The characteristic time for efflux τ_E is the average time constant calculated in CF efflux experiments with 1 μM peptide and 50 μM lipid concentrations. The experimental error (SD) in these values is ~ 20–50 %.

[e] TP10W, AGWLLGKINLKALAALAKKIL-amide. Data from ref.(6).

[f] N-terminal modifications: Acetyl (Ac), Rhodamine-Lissamine B (Rh).

[g] DL-1, formyl-MAQKIISTIGKLVKWIIKTVNKFTKK. Data from ref.(11). The Gibbs energies of transfer in DL-1, which is N-formylated, were calculated from those of acetylated peptides by subtracting the free energies of transfer of a methyl group from water to the interface (−1.1 kcal/mol) or to octanol (−1.9 kcal/mol) (31).

[h] a, C-terminal amidation.

[i] CE-2, KWKLLKKLEKAGAALKEGLLKAGPALALLGAAAALAK-amide. Data from ref.(11); τ_E was estimated by extrapolation from POPC/POPG mixtures with decreasing content of POPG.

Table 2

Summary of influx data in GUVs with Rh-TP10W, Rh-DL-1a, and CE-2.

	Rh-TP10W	Rh-DL-1a	CE-2
Independent GUV preparations	7	4	3
Number of assays	12	12	10
Number of outer GUVs examined	13	14	11
Number of inner GUVs examined	53	85	49
Inner GUVs with influx	35	21	3
Inner GUVs with influx in $t \leq 6\tau_o$	28	21	1
Percent of inner GUVs with influx in $t \leq 6\tau_o$	53 %	25 %	2 %